Physics Letters A ••• (••••) •••–•••

Contents lists available at ScienceDirect

Physics Letters A

www.elsevier.com/locate/pla

A metal-semiconductor transition triggered by atomically flat zigzag edge in monolayer transition-metal dichalcogenides

Yang Ni [a,b], Yan-Dong Guo [a,b,*], Xiao-Hong Yan [a,b,c,d,*], Hong-Li Zeng [e], Ying Zhang [c], Xin-Yu Chen [a], Xue-Yang Shen [a]

[a] College of Electronic and Optical Engineering, Nanjing University of Posts and Telecommunications, Nanjing 210023, China
[b] Key Laboratory of Radio Frequency and Micro-Nano Electronics of Jiangsu Province, Nanjing 210023, China
[c] College of Science, Nanjing University of Aeronautics and Astronautics, Nanjing 210016, China
[d] School of Material Science and Engineering, Jiangsu University, Zhenjiang, 212013, China
[e] College of Natural Science, Nanjing University of Posts and Telecommunications, Nanjing 210023, China

ARTICLE INFO

Article history:
Received 13 October 2018
Received in revised form 18 February 2019
Accepted 24 February 2019
Available online xxxx
Communicated by R. Wu

Keywords:
Transition-metal dichalcogenides (TMDs)
Density functional theory (DFT)
Atomically flat zigzag edge
Metal-semiconductor

ABSTRACT

Due to the structure of three stacked layers, monolayer transition-metal dichalcogenides (TMDs) is different from graphene. Creating atomically flat graphene-like edges in them has long been expected, which is crucial to the modulation of electronic structures in two-dimensional systems. Recently, by thermal annealing, Chen et al. [21] successfully synthesized atomically flat Mo-terminated edge in monolayer MoS_2. Inspired by this, through first-principles calculations, we studied the electronic and transport properties of typical TMD monolayers with transition atom-terminated flat zigzag edges, i.e., ScS_2, VS_2, CrS_2, FeS_2, NiS_2, MoS_2 and WS_2. It is found that the nanoribbons with and without flat edges are both metallic. Interestingly, the vacancy in the flat edge could open a transmission gap at the Fermi level in the ScS_2 ribbon, and trigger a metal-semiconductor transition. Further analysis shows that, the opening of bandgap around the Fermi level induced by the specific pattern of vacancies is the mechanism behind, which could be used as an modulating method for electronic structures. We believe our results are quite beneficial for the development of many other monolayer transition-metal dichalcogenides configurations, showing great application potential.

1. Introduction

Due to the peculiar properties originating from the reduction of dimensions, two-dimensional (2D) materials have been paid much attention in recent years [1–6]. For 2D materials, the edge is quite essential when they are reduced to nanoribbon widths. It could affect or even dominate the electronic, as well as the transport, properties of the whole system. More importantly, novel electronic, optical or magnetic properties might be triggered by the creation of the edge [7–10]. Previous studies showed that zigzag edge could transform graphene from a zero-band-gap semiconductor to a conductor, or even induce spontaneous magnetism [11,12]. Therefore, creating a edge could be used as an effective way to modulate the electronic structure of 2D materials.

Recent investigations have revealed that monolayer transition-metal dichalcogenides (TMDs) could provide electronic properties superior to that of graphene and other 2D materials [13]. They have received increasing research interest, and various applications have been proposed [14–17]. For example, Pan et al. [18,19] reported that VS_2 nanoribbons could be used as one-dimensional catalysts in electrolysis of water because of their catalytic abilities both on the basal planes and edges, and that the electronic and magnetic properties of MoS_2 nanoribbons could be controlled by applying strain, showing application potential in spintronics and photovoltaic cells. Because of the structure of three stacked layers, monolayer transition-metal dichalcogenides (TMDs) are different from graphene. Creating atomically flat graphene-like edges in them is crucial to the modulation of electronic structures, as well as the development of future devices. In addition, the atomically flat edge could also facilitate the investigation of further quantum phenomena in ribbons, e.g., weak localization [20,21]. However, the fabrication of such an edge has been rarely reported.

Recently, by high temperature annealing method, Chen et al. [21] successfully create large-scale atomically flat Mo-terminated zigzag edges in monolayer MoS_2 nanoribbons. Besides MoS_2, as far as we know, there are kinds of TMDs [13,22]. Such a method is ex-

* Corresponding authors.
E-mail addresses: yandongguo@njupt.edu.cn (Y.-D. Guo), xhyan@njupt.edu.cn (X.-H. Yan).

https://doi.org/10.1016/j.physleta.2019.02.032
0375-9601/

pected to be extended to many other TMD or even transition-metal chalcogenide systems, which also possess the sandwich structures. So, it is necessary to study the influence of the atomically flat edge on the electronic and transport properties of the TMD systems, which may facilitate the development of nanodevices.

In the present work, we focus on the TMD monolayers with transition atom-terminated flat zigzag edges, i.e., ScS_2-Sc, VS_2-V, CrS_2-Cr, FeS_2-Fe, NiS_2-Ni, MoS_2-Mo and WS_2-W, and study the electronic and transport properties of them, based on the density functional theory (DFT) combined with nonequilibrium Green's function (NEGF). It is found that all the nanoribbons possessing flat zigzag edges show finite transmission spectra at E_F, suggesting metallic. However, for ScS_2-Sc nanoribbon, the vacancy in the flat zigzag edge could open a gap at E_F in the transmission spectrum, transforming it into a semiconductor. Further analysis shows that, the opening of band gap around E_F induced by the pattern of vacancies is the mechanism underlying the metal-semiconductor transition. We believe such a method is quite beneficial for the development of many other monolayer transition-metal dichalcogenides configurations, showing great application potential.

2. Computational method

To investigate the electronic and the transport properties of the systems, we carry out our calculations with the Atomistix Toolkit package, based on the combination of density functional theory (DFT) and Green's function [23–25]. We use the mesh cut-off energy of 150 Ry, and the $1\times1\times150$ k-point mesh in the Monkhorst-Pack scheme is employed in the transport calculation [26]. The electron exchange correlation function is treated by generalized gradient approximation (GGA) in the form proposed by Perdew-Burke-Ernzerhof (PBE). [27,28] The supercell with sufficient vacuum spaces (more than 10 Å) in the x or y direction is chosen to eliminate the interactions between adjacent layers. The wave functions of all atoms are expanded using double-zeta plus polarization (DZP) basis set. To mimic the actual situation, the structures are fully relaxed until the force on each atom is less than 0.02 eV/Å.

In the present work, $T(E)$ is the transmission probability, which is obtained by (the denotation of spin is omitted)

$$T(E) = Tr[\Gamma_L(E)G^R(E)\Gamma_R(E)G^A(E)],$$

where $G^{R/A}(E)$ is the retarded/advanced Green's function of the scattering region, and $\Gamma_{L/R}$ is the coupling matrix to the left/right electrode.

3. Results and discussions

For TMD monolayers, it is reported that kinds of them could be synthesized [29,30]. In the present work, we focus on the monolayers of ScS_2, VS_2, CrS_2, FeS_2, NiS_2, MoS_2 and WS_2, which are proved to be stable in H structure [13]. They share the same hexangular sandwich structures. The transition metal atoms reside in the middle layer.

In order to obtain a flat edge, the bulk monolayer has to be cut into nanoribbons. In experiment, by high temperature annealing method, Chen et al. [21] successfully synthesized monolayer MoS_2 nanoribbons which possess large-scale atomically flat Mo-terminated zigzag edges, and found they can stably exist in room temperature. As the stability of nanoribbons is quite important to the practical application, in the present work, we performed the geometric optimization for all the cases investigated with the maximal force of 0.02 eV/Å. During the optimization, firstly, the nanoribbons with perfect flat Sc-terminated zigzag edges are constructed and optimized. Then, based on these configurations, we next construct the nanoribbons with Sc vacancies and optimize these geometries again, to ensure the most stable structure could be obtained.

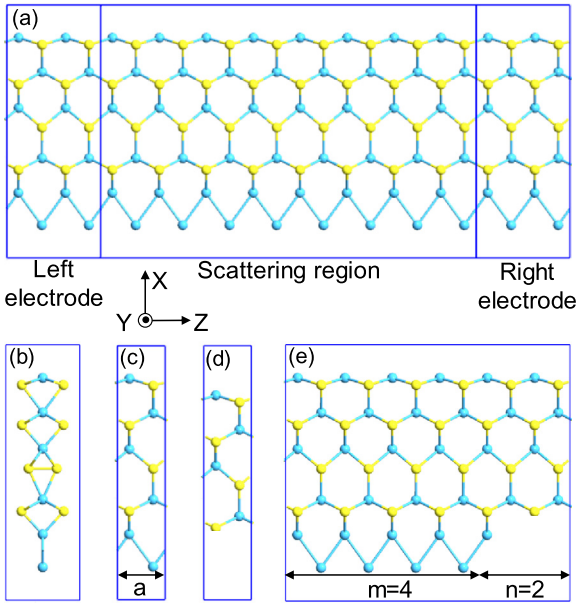

Fig. 1. (a) The two-probe configuration of ScS_2-Sc nanoribbon which possesses an atomically flat zigzag Sc edge. (b) Side view of ScS_2-Sc. (c) The cell of ScS_2-Sc. a is the lattice parameter in the Z direction. (d) The structure of ScS_2 nanoribbon. (e) The structure of ScS_2-Scmn, where a part of the Sc edge with n atoms length is missing. Here, m=4 and n=2.

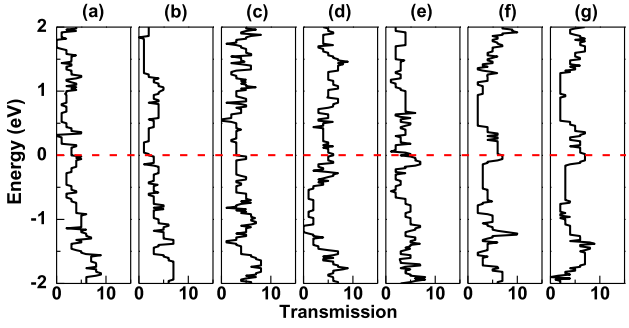

Fig. 2. (a)-(g) The transmission spectra of ScS_2-Sc, VS_2-V, CrS_2-Cr, FeS_2-Fe, NiS_2-Ni, MoS_2-Mo and WS_2-W, respectively. The Fermi level is set to be zero. The lattice parameters in the Z direction for the cells, are 3.70, 3.09, 2.97, 3.07, 3.40, 3.12 and 3.13 Å, respectively.

To investigate their electronic transport, we construct two-probe configurations. As an example, the two-probe setup of ScS_2-Sc is shown in Fig. 1(a). It consists of left/right electrode and the scattering region. One finds the Sc-Sc bond is much longer than that of Sc-S. From the side view of the geometry in Fig. 1(b), we can find that the bottom zigzag edge is quite flat. It should be noted that, according to the geometry of the TMDs, only one transition metal-terminated flat zigzag edge can be formed, showing the bottom of the nanoribbon in Fig. 1(a). Such an edge can not be formed on the other side of the ribbon, which we have confirmed by structural optimization with DFT calculations. And this is consistent with the experimental results [21].

To reveal the transport properties, we calculate the transmission spectra for all the configurations. Fig. 2 shows them for ScS_2-Sc, VS_2-V, CrS_2-Cr, FeS_2-Fe, NiS_2-Ni, MoS_2-Mo and WS_2-W, respectively. The lattice parameters in the Z direction for the cells of ScS_2, VS_2, CrS_2, FeS_2, NiS_2, MoS_2 and WS_2 are 3.70, 3.09, 2.97, 3.07, 3.40, 3.12 and 3.13 Å, respectively. The lattice parameter in the X direction is 40 Å, and the lattice parameter in the Y direction

Please cite this article in press as: Y. Ni et al., A metal-semiconductor transition triggered by atomically flat zigzag edge in monolayer transition-metal dichalcogenides, Phys. Lett. A (2019), https://doi.org/10.1016/j.physleta.2019.02.032

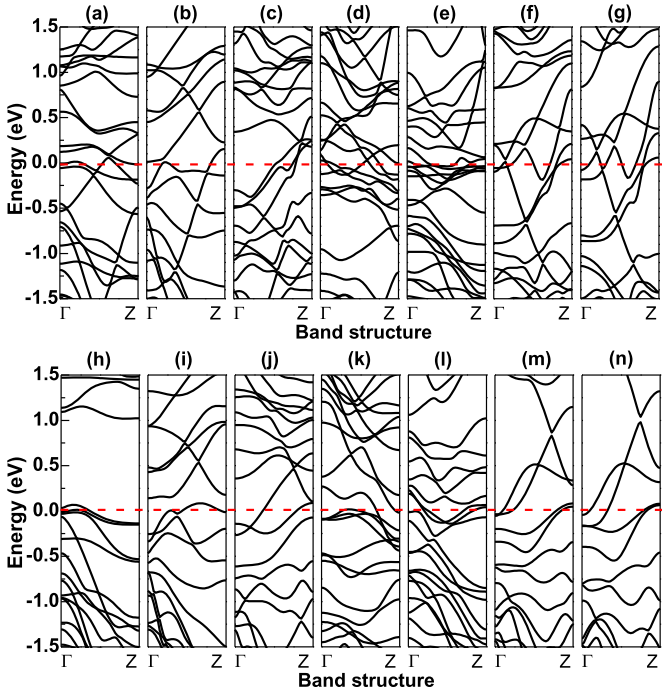

Fig. 3. (a)-(g) The band structures of ScS_2-Sc, VS_2-V, CrS_2-Cr, FeS_2-Fe, NiS_2-Ni, MoS_2-Mo and WS_2-W, respectively. Each nanoribbon possesses an atomically flat zigzag edge. (h)-(n) The band structures of ScS_2, VS_2, CrS_2, FeS_2, NiS_2, MoS_2 and WS_2, respectively (the same order with that of (a)-(g)). There is no atomically flat zigzag edge in each nanoribbon.

is 20 Å. The vacuum spaces of the supercell in the X and Y directions are both sufficient (more than 10 Å). One finds, at the Fermi level (0 eV), all the transmission coefficients are finite. That is to say, they are all metallic. And the transmission coefficients are all larger than 2.0 and even reach 7.0. Thus, there are more than one transmission eigenchannels for every case. In other words, there is no transmission gap for all the configurations.

The relationship between band structure and transmission spectrum likes that between band structure and density of states (DOS). Although transmission spectrum or DOS may not provide additional information, the presentation of them could facilitate the analysis of the electronic structure, offering another perspective on the data. So we calculate the band structures for all the nanoribbons to gain insight into the transmission spectra. Fig. 3(a)-(g) show the band structures of ScS_2-Sc, VS_2-V, CrS_2-Cr, FeS_2-Fe, NiS_2-Ni, MoS_2-Mo and WS_2-W, respectively. One finds for all of them, there are more than one band across the Fermi level. It is these bands that contribute to the transmission around E_F in Fig. 2. Note that none of the ribbons exhibits semiconductor behavior. However, in practical applications, semiconductor feature is needed.

To figure out the influence of the flat zigzag edge on the system, we calculate the band structures of the monolayers without the flat edge. Fig. 1(d) shows the structure of ScS_2, which does not possess that edge. And Fig. 3(h)-(n) give out the band structures of ScS_2, VS_2, CrS_2, FeS_2, NiS_2, MoS_2 and WS_2, respectively. For all of them, there are several bands across the Fermi level. They are all metallic, the same like those possessing flat edges. For some cases, the number of bands across E_F changes, compared with the ribbon with flat edge. For instance, there are two and three bands before and after adding the flat edge for CrS_2, see Fig. 3(j) and (c) respectively. From the metal-semiconductor transition point of view, the perfect flat zigzag edge have little effect.

However, the ScS_2 nanoribbon is different from others. Although it is metallic, there is a wide band gap above E_F, see

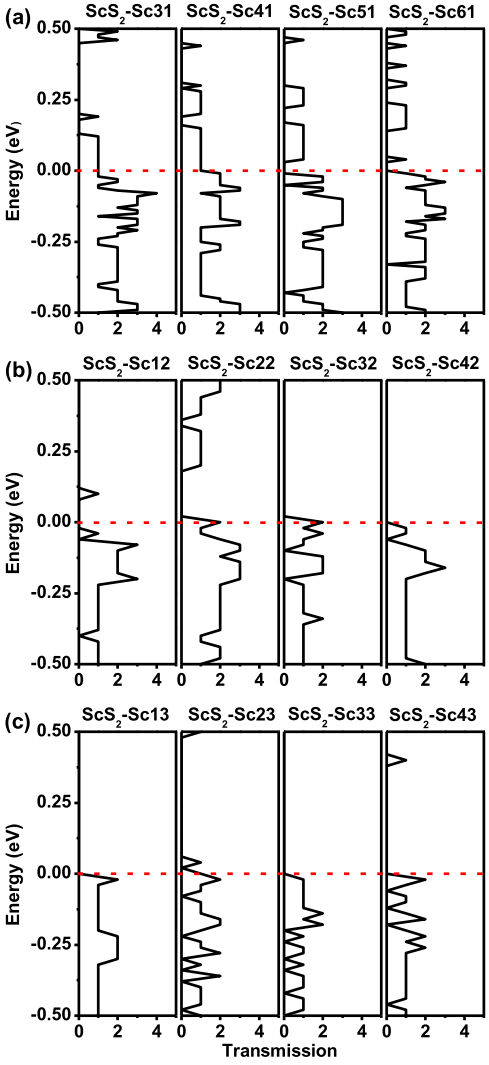

Fig. 4. The transmission spectra for ScS_2-Scmn. (a) m=3, 4, 5 and 6; n=1. (b) m=1, 2, 3 and 4; n=2. (c) m=1, 2, 3 and 4; n=3.

Fig. 3(h). Compared with that of ScS_2-Sc in Fig. 3(a), one finds that the introduction of flat edge induces more bands, which fills up the band gap. Such a band gap feature may provide us a way to modulate the electronic structure in these ribbon systems, as the transition state between ScS_2 and ScS_2-Sc nanoribbons may trigger interesting electronic properties.

In geometry, ScS_2-Sc nanoribbon is full of flat edge on one side, but ScS_2 is not. Between these two configurations, there would be transition structures which possess vacancies on the flat edge. For clarity, we here define two parameters, i.e., m and n, which represents the lengths of the flat edge part and the vacancy part respectively. Fig. 1(e) shows the structure of one such configuration, where m=4 and n=2. Finally, a transition configuration is denoted by ScS_2-Scmn. Through the optimization under DFT calculations, this kind of configurations are proved to be stable.

To fully investigate the effect of the edge vacancy, we construct a series of configurations with varied m and n. Fig. 4 shows the transmission spectra of them. First, we construct one vacancy (n=1) and change m in a cell. Fig. 4(a) shows the transmission spectra of ScS_2-Scm1, where m=3, 4, 5 and 6. When m=3 or 4, the transmission coefficient is finite at E_F, suggesting these configurations are metallic. It is easy to understand as the ScS_2 and ScS_2-Sc nanoribbons are both metallic, which can be seen as the "parents" of these structures. Moreover, there are transmission gaps above

Please cite this article in press as: Y. Ni et al., A metal-semiconductor transition triggered by atomically flat zigzag edge in monolayer transition-metal dichalcogenides, Phys. Lett. A (2019), https://doi.org/10.1016/j.physleta.2019.02.032

the Fermi level for them. Interestingly, when m=5 or 6, there is a transmission gap at the Fermi energy. In other words, the nanoribbon change to semiconductors when m=5 or 6. The semiconducting behavior does not exist in ScS_2 or ScS_2-Sc nanoribbon. So the metal-semiconductor transition is quite interesting. Besides, there are also tiny gaps above E_F, similar to ScS_2-Sc31 and ScS_2-Sc41.

When n=2, the vacancy part becomes larger. And there are both metallic and semiconducting configurations. From Fig. 4(b), one finds there is a transmission gap emerging at E_F for ScS_2-Sc12 or ScS_2-Sc42 system, suggesting they become semiconductors. As for ScS_2-Sc22 and ScS_2-Sc32, they are still metallic. Similarly, there are also some other transmission gaps above E_F. Interestingly, compared with the ScS_2-Scm1 cases in Fig. 4(a), the gaps above E_F become wider. When n increases further to 3, the three configurations of ScS_2-Sc13, ScS_2-Sc33 and ScS_2-Sc43 become semiconductors, but ScS_2-Sc23 is metallic, see Fig. 4(c). Apparently, the atomically flat zigzag transition metal-terminated edge is quite essential to the electronic transport of ScS_2-based systems. A slight change in edge structure could trigger the metal-semiconductor transition, which would be rather beneficial to the development of nanoelectronic devices when the minimization goes further. In brief, such a method could be used to modulate the electronic structure of the ScS_2 systems. Moreover, it is expected to be extended to many other similar sandwiched geometry systems, such as transition-metal chalcogenides, showing great application potential.

To trace the origin of the transmission spectra, we calculate the band structures for all the ScS_2-Scmn ribbons above, shown in Fig. 5. The band structures in Fig. 5 corresponds to the transmission spectra one-to-one respectively. One finds, when n=1, there are bands across the Fermi level for ScS_2-Sc31 and ScS_2-Sc41 nanoribbons, but not for ScS_2-Sc51 and ScS_2-Sc61 ones. That is to say, the former two configurations are metallic and the latter two are semiconducting. Obviously, for the former two, it is the bands that across E_F contribute to the finite transmission around the Fermi energy in the transmission spectra, showing Fig. 4(a). For the latter two, the missing of band at E_F results in the transmission gaps in the transmission spectra of ScS_2-Sc51 and ScS_2-Sc61, showing Fig. 4(a). So, the band structures are the origin of the transmission spectra. Similarly, we can do the same analysis for the n=2 and n=3 cases, and the same mechanism are found that the transmission spectra is resulted from the band structures.

For the configurations of ScS_2-Scmn, where mn denotes 51, 61, 12, 42, 13, 33 and 43, we plot the orbitals of valence-band maximum (VBM) and conduction-band minimum (CBM), shown in Fig. 6. One easily finds both the VBM and CBM orbitals distribute on (or near) the edge. For the VBM ones, some distribute on (or near) the upper edge and some distribute on (or near) the lower edge. However, the CBM orbitals all distribute on (or near) the lower edge, i.e., the atomically flat Sc-terminated zigzag edge, except that of ScS_2-Sc43 which distributes on both edges.

In graphene, both experimental and theoretical studies have shown that the confinement originating from periodic lattice perturbations can induce band gap opening [31–34]. From the structural point of view, our configurations, in particular the flat edge part, could be seen as the superlattice systems. Due to the similar flat hexangular geometry, confinement-induced gap opening by superlattice structure could be expected. Actually, for our systems, almost every configuration opens an energy gap around the Fermi level, except ScS_2-Sc31 and ScS_2-Sc41, see Fig. 4. Interestingly, all the energy gaps are above the Fermi level (or most part of the gap lies above E_F), and none gap appears below the Fermi level (or only a small part of the gap exists under E_F). In other words, for these gaps, the position of their bottom in the energy axis is fixed (very close to E_F). Thus, (the size of) the energy gap is mainly determined by the CBM. This is consistent with the above analysis,

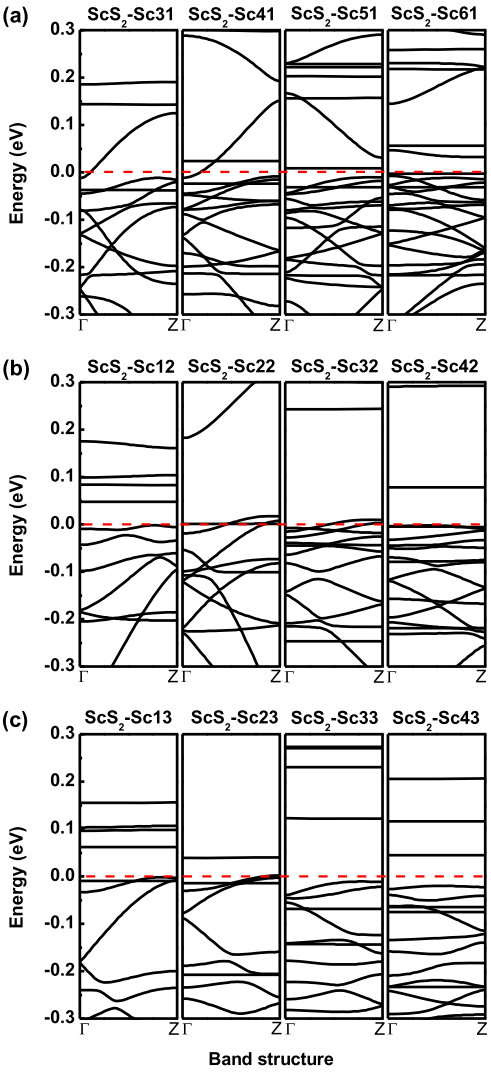

Fig. 5. The corresponding band structures for Fig. 4.

where we found the CBM orbitals all distribute on (or near) the lower edge. And, this flat edge with vacancies is exactly the origin of the periodic lattice perturbations. So, the confinement of the superlattice feature lead to the distribution of the CBM orbital and finally results in the band gap.

It should be noted that, for n=1 cases, the configurations of ScS_2-Sc11 and ScS_2-Sc21 are also calculated. But they are not shown here, as they are metallic, just like ScS_2-Sc31 and ScS_2-Sc41. In the present work, we focus on the transition from metallic to semiconducting, which happens between ScS_2-Sc41 and ScS_2-Sc51.

4. Conclusion

In summary, based on first-principles calculations, we studied the electronic and transport properties of typical TMD monolayers with transition atom-terminated flat zigzag edges, i.e., ScS_2-Sc, VS_2-V, CrS_2-Cr, FeS_2-Fe, NiS_2-Ni, MoS_2-Mo and WS_2-W. It is found that all these nanoribbons with flat zigzag edges are metallic. Interestingly, the vacancy in the flat zigzag edge could open a transmission gap at the Fermi level in the ScS_2-Sc ribbon, and induce a metal-semiconductor transition. Further analysis shows that, the opening of bandgap around E_F induced by the vacancy is the mechanism behind. This could be used as an effective way to modulate the electronic structure of the ribbon. Moreover, it is ex-

Please cite this article in press as: Y. Ni et al., A metal-semiconductor transition triggered by atomically flat zigzag edge in monolayer transition-metal dichalcogenides, Phys. Lett. A (2019), https://doi.org/10.1016/j.physleta.2019.02.032

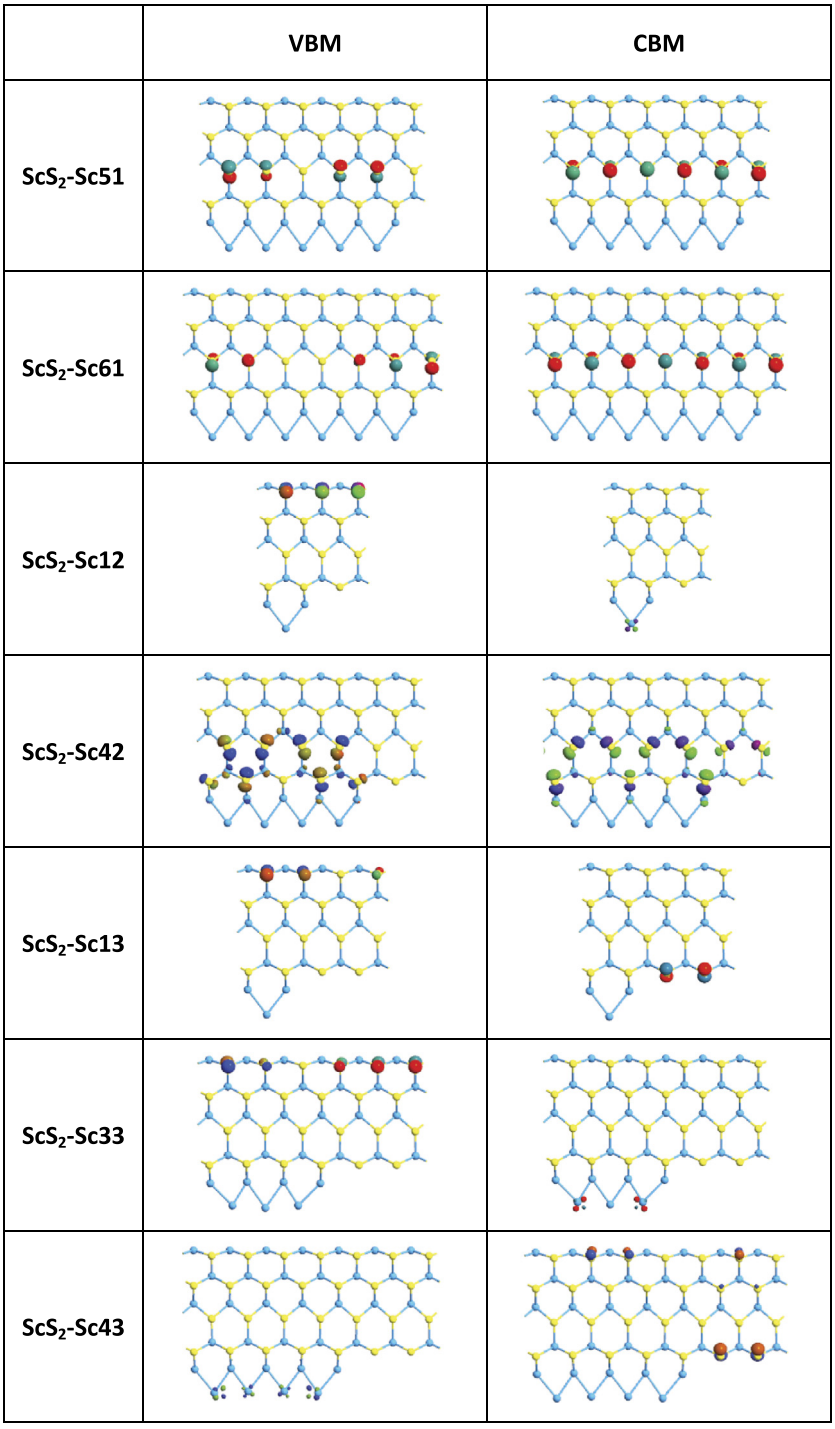

Fig. 6. The orbitals of valence-band maximum (VBM) and conduction-band minimum (CBM) of ScS_2-Scmn.

pected to be extended to many other transition-metal chalcogenide systems, showing application potential.

Acknowledgements

This work is supported by the National Natural Science Foundation of China (NSFC11705097, NSFC11504178 and NSFC11804158), the Natural Science Foundation of Jiangsu Province (BK20150825 and BK20170895), the Scientific Research Foundation of Nanjing University of Posts and Telecommunications (NY217013 and NY214151), and Natural Science Fund for Colleges and Universities in Jiangsu Province (17KJB140015).

References

[1] S. Stankovich, D.A. Dikin, R.D. Piner, K.A. Kohlhaas, A. Kleinhammes, Y. Jia, Y. Wu, S.T. Nguyen, R.S. Ruoff, Synthesis of graphene-based nanosheets via chemical reduction of exfoliated graphite oxide, Carbon 45 (7) (2007) 1558–1565.

[2] Y.D. Guo, X.H. Yan, Y. Xiao, Electrical control of the spin polarization of a current in pure-carbon systems based on partially hydrogenated graphene nanoribbon, J. Appl. Phys. 113 (24) (2013) 244302.

[3] Y.D. Guo, X.H. Yan, Y. Xiao, Spin-polarized current generated by carbon chain and finite nanotube, J. Appl. Phys. 108 (10) (2010) 104309.

[4] H.C. Schniepp, J.-L. Li, M.J. McAllister, H. Sai, M. Herrera-Alonso, D.H. Adamson, R.K. Prud'homme, R. Car, D.A. Saville, I.A. Aksay, Functionalized single graphene sheets derived from splitting graphite oxide, J. Phys. Chem. B 110 (17) (2006) 8535–8539.

Please cite this article in press as: Y. Ni et al., A metal-semiconductor transition triggered by atomically flat zigzag edge in monolayer transition-metal dichalcogenides, Phys. Lett. A (2019), https://doi.org/10.1016/j.physleta.2019.02.032

[5] M.Y. Han, B. Özyilmaz, Y. Zhang, P. Kim, Energy band-gap engineering of graphene nanoribbons, Phys. Rev. Lett. 98 (20) (2007) 206805.
[6] M.X. Chen, M. Weinert, Half-metallic Dirac cone in zigzag graphene nanoribbons on graphene, Phys. Rev. B 94 (3) (2016).
[7] K. Nakada, M. Fujita, G. Dresselhaus, M.S. Dresselhaus, Edge state in graphene ribbons: nanometer size effect and edge shape dependence, Phys. Rev. B 54 (24) (1996) 17954.
[8] Y. Kobayashi, K.-i. Fukui, T. Enoki, K. Kusakabe, Edge state on hydrogen-terminated graphite edges investigated by scanning tunneling microscopy, Phys. Rev. B 73 (12) (2006) 125415.
[9] H. Pan, Y.W. Zhang, Edge-dependent structural, electronic and magnetic properties of mos2 nanoribbons, J. Mater. Chem. 22 (15) (2012) 7280–7290.
[10] Y.-W. Son, M.L. Cohen, S.G. Louie, Energy gaps in graphene nanoribbons, Phys. Rev. Lett. 97 (21) (2006) 216803.
[11] X. Cong, Y. Liao, Q. Peng, Y. Yang, C. Cheng, W. Zhang, P. Fang, C. Chen, L. Miao, J. Jiang, Contrastive band gap engineering of strained graphyne nanoribbons with armchair and zigzag edges, RSC Adv. 5 (73) (2015) 59344–59348.
[12] Y.Y. Li, M.X. Chen, M. Weinert, L. Li, Direct experimental determination of onset of electron–electron interactions in gap opening of zigzag graphene nanoribbons, Nat. Commun. 5 (44) (2014) 4311.
[13] C. Ataca, H. Sahin, S. Ciraci, Stable, single-layer mx2 transition-metal oxides and dichalcogenides in a honeycomb-like structure, J. Phys. Chem. C 116 (116) (2012) 8983.
[14] C. Tan, Two-dimensional transition metal dichalcogenide nanosheet-based composites, Chem. Soc. Rev. 44 (9) (2015) 2713–2731.
[15] M.M. Ugeda, A.J. Bradley, S.F. Shi, J.F. Da, Y. Zhang, D.Y. Qiu, W. Ruan, S.K. Mo, Z. Hussain, Z.X. Shen, Giant bandgap renormalization and excitonic effects in a monolayer transition metal dichalcogenide semiconductor, Nat. Mater. 13 (12) (2014) 1091–1095.
[16] T. Jakubczyk, K. Nogajewski, M.R. Molas, M. Bartos, W. Langbein, M. Potemski, J. Kasprzak, Impact of environment on dynamics of exciton complexes in a ws_2 monolayer, 2D Mater. 5 (2017) 031007.
[17] J. Kim, S. Byun, A.J. Smith, J. Yu, J. Huang, Enhanced electrocatalytic properties of transition-metal dichalcogenides sheets by spontaneous gold nanoparticle decoration, J. Phys. Chem. Lett. 4 (8) (2013) 1227–1232.
[18] H. Pan, Y.W. Zhang, Tuning the electronic and magnetic properties of mos2 nanoribbons by strain engineering, J. Phys. Chem. C 116 (21) (2012) 11752–11757.
[19] Y. Qu, H. Pan, C.T. Kwok, Z. Wang, A first-principles study on the hydrogen evolution reaction of vs2 nanoribbons, Phys. Chem. Chem. Phys. 17 (38) (2015) 24820.
[20] G. Bergmann, Weak localization in thin films: a time-of-flight experiment with conduction electrons, Phys. Rep. 126 (1) (1984) 229–234.
[21] Q. Chen, H. Li, W. Xu, S. Wang, H. Sawada, C.S. Allen, A.I. Kirkland, J.C. Grossman, J.H. Warner, Atomically flat zigzag edges in monolayer mos2 by thermal annealing, Nano Lett. 17 (9) (2017) 5502–5507.
[22] P. Cui, J.H. Choi, W. Chen, J. Zeng, C.K. Shih, Z. Li, Z. Zhang, Contrasting structural reconstructions, electronic properties, and magnetic orderings along different edges of zigzag transition metal dichalcogenide nanoribbons, Nano Lett. 17 (2) (2017) 1097.
[23] M. Brandbyge, J.-L. Mozos, P. Ordejón, J. Taylor, K. Stokbro, Density-functional method for nonequilibrium electron transport, Phys. Rev. B 65 (16) (2002) 165401.
[24] J. Taylor, H. Guo, J. Wang, Ab initio modeling of quantum transport properties of molecular electronic devices, Phys. Rev. B 63 (24) (2001) 245407.
[25] A.J. Cohen, P. Mori-Sánchez, W. Yang, Insights into current limitations of density functional theory, Science 321 (5890) (2008) 792–794.
[26] H.J. Monkhorst, J.D. Pack, Special points for Brillouin-zone integrations, Phys. Rev. B 13 (12) (1976) 5188–5192.
[27] J.P. Perdew, K. Burke, M. Ernzerhof, Generalized gradient approximation made simple, Phys. Rev. Lett. 77 (18) (1996) 3865–3868.
[28] J.P. Perdew, J.A. Chevary, S.H. Vosko, K.A. Jackson, M.R. Pederson, D.J. Singh, C. Fiolhais, Atoms, molecules, solids, and surfaces: applications of the generalized gradient approximation for exchange and correlation, Phys. Rev. B 46 (11) (1992) 6671.
[29] R. Lv, J.A. Robinson, R.E. Schaak, D. Sun, Y. Sun, T.E. Mallouk, M. Terrones, Transition metal dichalcogenides and beyond: synthesis, properties, and applications of single- and few-layer nanosheets, Acc. Chem. Res. 48 (1) (2015) 56–64.
[30] Y. Shi, H. Li, L. Li, Recent advances in controlled synthesis of two-dimensional transition metal dichalcogenides via vapour deposition techniques, Chem. Soc. Rev. 44 (9) (2015) 2744–2756.
[31] R. Balog, B. Jørgensen, L. Nilsson, M. Andersen, E. Rienks, M. Bianchi, M. Fanetti, E. Laegsgaard, A. Baraldi, S. Lizzit, Bandgap opening in graphene induced by patterned hydrogen adsorption, Nat. Mater. 9 (4) (2010) 315.
[32] L. Chernozatonskiĭ, P.B. Sorokin, E. Belova, J. Brüning, A.S. Fedorov, Superlattices consisting of “lines” of adsorbed hydrogen atom pairs on graphene, JETP Lett. 85 (1) (2007) 77–81.
[33] E.J. Duplock, M. Scheffler, P.J.D. Lindan, Hallmark of perfect graphene, Phys. Rev. Lett. 92 (2004) 225502.
[34] T.G. Pedersen, F. Christian, P. Jesper, M. Niels Asger, J. Antti-Pekka, P. Kjeld, Graphene antidot lattices: designed defects and spin qubits, Phys. Rev. Lett. 100 (13) (2008) 136804.

Please cite this article in press as: Y. Ni et al., A metal-semiconductor transition triggered by atomically flat zigzag edge in monolayer transition-metal dichalcogenides, Phys. Lett. A (2019), https://doi.org/10.1016/j.physleta.2019.02.032